Impact of geometrical resolution on long-term climate-based daylight metrics

Forouzandeh, Nima; Brembilla, Eleonora; Stoter, Jantien; Nan, L.

DOI
10.26868/25222708.2023.1132

Publication date
2024

Document Version
Final published version

Published in
Proceedings of Building Simulation 2023

Citation (APA)
Forouzandeh, N., Brembilla, E., Stoter, J., & Nan, L. (2024). Impact of geometrical resolution on long-term climate-based daylight metrics. In *Proceedings of Building Simulation 2023: 18th Conference of IBPSA* (pp. 698-704). (Building Simulation Conference proceedings). IBPSA. https://doi.org/10.26868/25222708.2023.1132

Impact of geometrical resolution on long-term climate-based daylight metrics

Nima Forouzandeh[1], Eleonora Brembilla[1], Jantien Stoter[1], Liangliang Nan[1]
[1]Faculty of Architecture and the Built Environment,
Delft University of Technology, Delft, Netherlands

Abstract

3D modeling of indoor spaces is a prerequisite for daylight simulation, and the accuracy of the 3D models can have a significant impact on the simulation. The goal of this study was to quantify the errors caused by modeling indoor spaces at different accuracy levels to find the optimal balance between the reliability of the results and labor investment. For this purpose, we introduce a Level of Detail (LOD) concept for indoor spaces based on the size of non-permanent indoor objects by inclusion and exclusion from the simulation scene. The errors corresponding to models with low accuracies are measured on six case study offices by climate-based simulation using an improved two-phase method. Our results show that inaccurate modeling of indoor spaces can cause between 10%-70% error in Total Annual Illumination (TAI) with a 25% median across all spaces of our study.

Highlights

- We introduce a concept of level of detail for indoor daylight applications.
- Inaccurate modeling of indoor spaces causes between 10%-70% errors on climate-based daylight simulation results.
- Our study lays the theoretical ground for automation of 3D modelling for indoor daylight simulation.

Introduction

In the past decade, climate-based daylight modeling has become an integral component of daylight assessments in many national and international standards and certifications, e.g., LEED, UK Education Funding Agency (EFA), EN 17037(EN, 2019; EFA, 2014; USGBC, 2013).

The required geometrical level of detail for efficient daylight modeling of indoor space is not yet known for different applications, e.g., design, and post-occupancy evaluation, potentially leading to significant errors in final results and to design solutions that do not efficiently address building occupants' needs and requirements. This issue still requires a better understanding of what is optimum balance between performance, labour investment and accuracy.

Post-occupancy evaluation is a common means to understand the daylight performance and the design quality of a building in the post-construction phases of the building's life cycle. Such studies can inform retrofitting strategies, as well as forming a knowledge base to improve the planning and design of new buildings. Calibrated climate-based daylight models play a pivotal role in such evidence-based knowledge in the existing building stock (Quek and Jakubiec (2021)). Yet, given the large number of existing buildings, a standardization of 3-dimensional data acquisition and modeling techniques is essential for achieving this goal with minimum labor cost, since creating and preprocessing 3D models for daylight simulation can be labor-intensive. This, for the main part is attributed to the permanent structures of the spaces, e.g. walls, windows, ceiling, but in most indoor spaces the effort of surveying all furniture is even heavier. Several studies have been targeting the optimization of such a 3-dimensional representation of the building for the intended spatial analysis. The concept of Level of Detail (LOD), for instance, is developed in 3D city modeling for efficient representation of the building depending on the intended use. The idea of LOD has extensively been studied and applied in urban-level 3D modeling of buildings to balance the acquisition and reconstruction cost with respect to the desired application requirements (Biljecki et al. (2016); Kutzner et al. (2020)).

On the contrary, for indoor spatial analyses, the existing literature is more limited and there are still many open questions that research needs to answer. Boeters et al. (2015) proposed an enhancement for CityGML LOD2 for area determination. Kim et al. (2014) studied the possible integration of IndoorGML with CityGML. (Billen et al., 2012) proposed 3 LODs for developing the CityGML v2.0(OGC, 2012). Kemec et al. (2012) proposed additional indoor LoDs of 1.5, 2.5, and 3.5 with corresponding buildings objects of story, compartment, and apartment, respectively to be applied to natural disaster risk communication purposes. Hagedorn et al. (2009) proposed an indoor LOD for route visualization by including three components of thematic models, geometry model, and routing model for indoor route visualization. Löwner et al. (2013) and Benner et al. (2013) proposed an expanded concept of interior LOD for CityGML by differentiating between geometrical LOD and Semantical LOD, separately for building interior and building exterior. Pang et al. (2020) suggested new LODs, consisting of three semantic levels (SLOD) including enclosing components, connecting components, and

https://doi.org/10.26868/25222708.2023.1132

decorating components. Besides semantic LODs, it also proposed geometric LOD (GLOD) and evolutionary processes (PLOD). Following a similar approach, Kang et al. (2018) defined indoor LOD by defining position accuracy (PLOD), geometric (GLOD), completeness (CLOD), and semantics (SLOD), and focuses on the requirements for indoor disaster management service. Boeters et al. (2015) proposed interior LOD corresponding to exterior LOD2 with comparable complexity and a methodology for automatically generating them from an existing exterior model with LOD2.

Geiger et al. (2015) investigated and described the concept of generating generalized representations, i.e., representations with lower LOD suitable for regional and urban levels (transforming BIM to GIS), for buildings and building elements in BIM format based on the LOD concept of CityGML.

The above studies all propose definitions that suit a particular application and are not applicable to other types of indoor physical and spatial analyses, e.g., indoor daylight analysis, which is the focus of this study.

To address the lack of established LODs for indoor daylight analysis, it is crucial to quantify errors in results stemming from simplified geometric models. This study aims to fill this gap by measuring errors that arise when non-permanent objects, such as chairs, tables, and screens, are excluded from the model based on their size. The results of this study will be useful to propose LOD framework suitable for indoor daylight applications in order to optimize between performance, labor investment, and reliability of results, and to understand the errors caused by inaccurate geometry definitions.

Methods

Spaces and input preparation

In this study, we select six large open office spaces located in Singapore, previously modeled for a study on validation and calibration of climate-based daylight simulation (Quek and Jakubiec (2021)). A representation of these spaces is shown in Fig. 1.

To generate a daylight model of a given space, 10 threshold levels are calculated for each non-permanent object based on their oriented bounding box area. An oriented bounding box is simply a bounding volume whose faces and edges are not parallel to the basis vectors of the coordinate system in which they are defined. The threshold levels are determined using a uniform distribution within the size range of the non-permanent objects in the space. The size ranges in each space is presented in Fig. 2 . For each threshold level, a corresponding daylight model is generated. The model only includes non-permanent objects whose oriented 3D bounding area size exceeds the threshold value. Therefore, as the threshold value increases, the geometrical resolution of the model decreases.

Daylight simulation and evaluated metrics

The Radiance improved 2-phase method was chosen to run annual daylight simulations, using the Radiance rendering engine (Ward, 1994). Improved (Dynamic Daylight Simulation (DDS)) distinguishes between the contribution of various sources, including diffuse sky, diffuse ground, indirect solar component, and direct solar component. For the last component, the number of positions can be defined as higher for a better accuracy, resulting in a more realistic representation. This method is suitable for buildings without complex fenestration systems which is the case for the buildings in our study (Bourgeois et al., 2008). For each model, we ran a climate-based daylight simulation and calculated the Total Annual Illumination (TAI) and Daylight Autonomy (DA). TAI or light exposure is calculates as the sum of all the illuminance values in the occupancy hours throughout the year. DA is defined as the percentage of occupied hours that a point in the space receives more light than a certain threshold, in our case 300 lux. The grid points are placed at 0.8m level, pointing upwards. We ensured that the nodes covered by the furniture pieces were removed to avoid bias in the results. Spaces are assumed to be occupied throughout the whole year and not just in the office hours.

Results and discussion

The Absolute Percentage Error (APE)s by size-wise exclusion at each of the objects is shown in Fig. 6 for three of the spaces. The errors expectably increase by an increase in the exclusion threshold value, however, the error range differs among different datasets, e.g., maximum APE on mean TAI of 15% for S2 and 27% for S4 (Fig. 7).

In space S0, removing objects with sizes smaller than the first threshold of $7m^2$, resulted in a 37% decrease in TAI and a 5% decrease in mean DA. These percentages were nearly as high as the maximum error observed in both metrics. This behavior is due to the uniform size threshold definition used in the experiment and the high variability of object sizes, as depicted in Fig.3. The removal of many furniture pieces located near grid points during the first step, because of their small size, contributed significantly to the observed changes in TAI and mean DA.

https://doi.org/10.26868/25222708.2023.1132

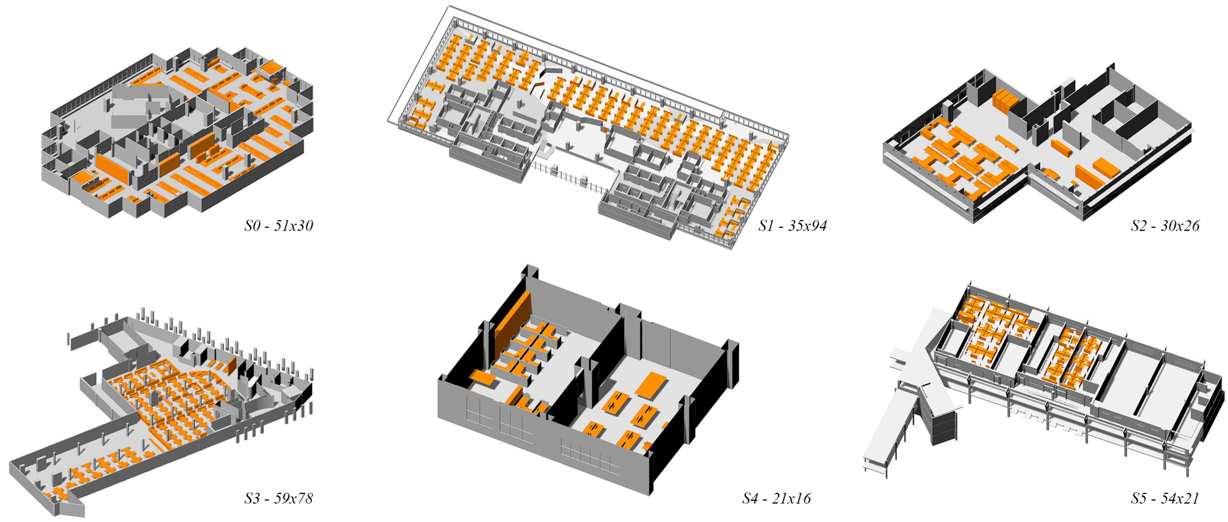

Figure 1: The indoor datasets used in this study, from S0 (top-left) to S5(bottom-right), the non permanent indoor objects are highlighted in orange. Room dimensions are in meters.

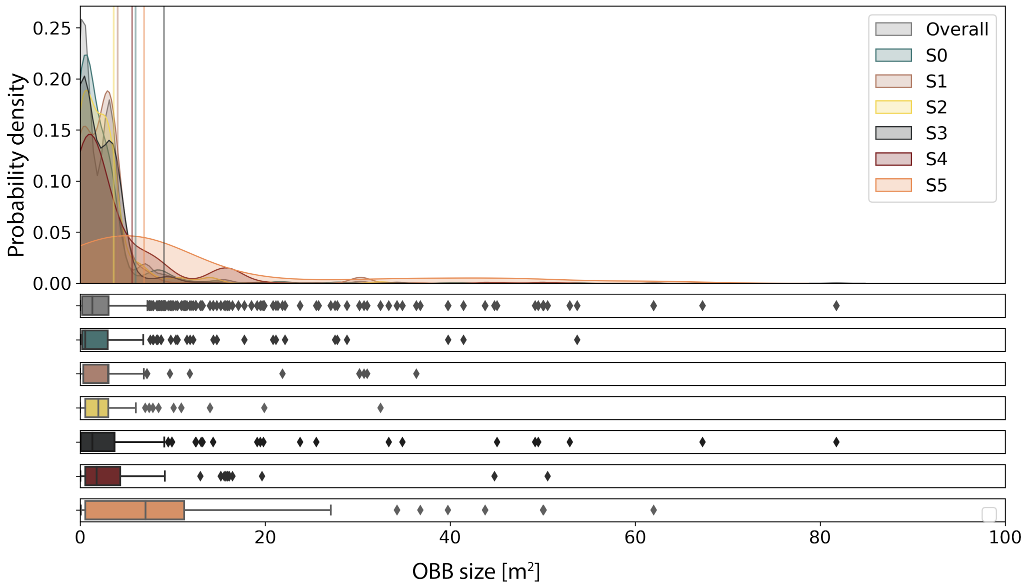

Figure 2: Size distribution of furniture across the six indoor datasets, vertical lines show the first threshold for each dataset.

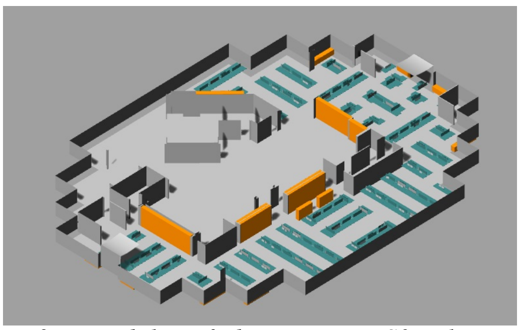

Figure 3: Variability of object sizes in S0. The smaller-sized objects with higher occurrences are highlighted in blue, and the sparsely located large objects are depicted in orange.

The same trend occurs in S1, with a maximum error of 28% for TAI and 4% for mean DA, where the majority of the indoor objects fall within the first size bounds and their exclusion causes significant errors in the annual results. Note that mean DA remains almost constant in S0 and S1 due to the definition of this metric, which behaves equally with all the nodes receiving more than 300lux at each hour throughout the occupancy hours in a year.

In space S2, the APE for TAI, is 15% and the APE for DA is 10%. The rise in error is gradual and consistent between steps. On the last threshold removing the large shelves located close to the window surfaces (left side of the space, see 1) causes a 4-5% increase in the errors. The same behavior is observed, in some of the other spaces

https://doi.org/10.26868/25222708.2023.1132

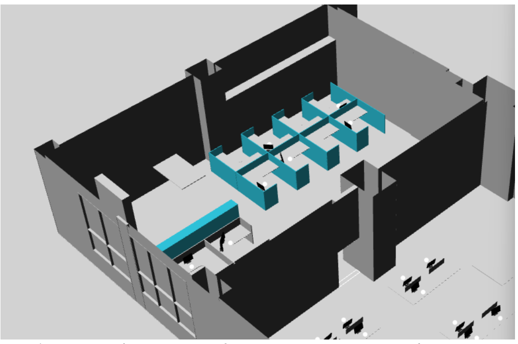

Figure 4: Visualisation of non-permanent objects causing a sudden increase in the errors in space S4, highlighted in blue.

on the first threshold where a high number of relatively smaller-sized objects are removed from the 3D model.

Step-wise removal of the objects in S3, being one of the largest open offices relative to the others, led to a maximum error of 15% for mean DA and 13% for TAI. The increase in error in the first threshold is steep, with an increase of 8% for mean DA and 6% for TAI. Throughout the rest of the iterations, the changes in the error rate are almost constant.

In S4, a smaller-sized open office, after the first step, a small increase was observed with a 4% difference in TAI and 8% in mean DA. However, a larger increase occurred in the third step when desk partitions and a large shelf located close to the windows were removed from the space, as shown in Fig.4. This increase can be attributed to both the size of the objects and their proximity to the windows, which cast shadows on the work-plane grids.

In S5, the errors are considerably higher than in the other spaces, with a 70% error rate for TAI and an 80% error rate for mean DA. The sudden increases observed in the final thresholds were caused by removing the partitions that surrounded the grid points on the working plane, as illustrated in Fig. 5. The same applies to space S4.

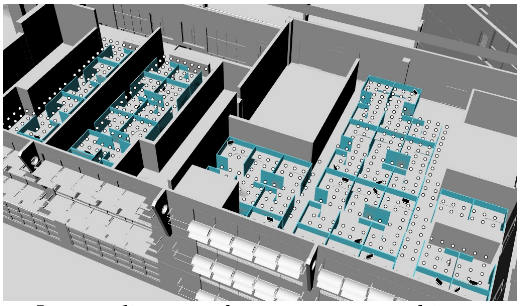

Figure 5: Visualisation of non-permanent objects causing a sudden increase in the errors in space S5, shown in blue, along with the grid points.

A summary of the distribution of the APEs after the exclusion of objects at each of the nine steps is presented in Fig.7 (top), showing that incomplete modeling of furniture can lead to up to 70% error in TAI. Fig.7 (middle) shows the distribution of the contributions for each step across the models or the steepness of the curve slopes at each step in the top-row plots in Fig.6. The number of the objects is shown in the bottom plot in Fig.7.

Looking at the step-wise errors (Fig. 7- middle) one could see that a noticeable portion of the total error occurs in the first step, which based on the frequency of the objects at each size-step (Fig. 7- middle and bottom) is where 78-98% of objects are placed. These plots show that there exists a threshold in all the models, which is meaningful for daylight calculations. Exclusion of objects falling below that threshold, according to these plots, will lead to a minor error in the calculation of total annual illumination. Furthermore, that threshold is around the first step for each dataset, which can be explained by the high number of occurrences of furniture pieces in that range (Fig.7 middle and Fig.2). The first threshold value is between 5 and 11 m^2 depending on the dataset as shown in Fig.2. More datasets and simulations are required in order to provide accurate size recommendations for daylight applications, which will be done in our future work.

The office buildings in this study vary in terms of size and window sides to be representative of open office spaces, as such, this approach is limited to office spaces. This is crucial for understanding how to interpret the study's findings because in other building types, the types of non-permanent objects and, consequently, their sizes can change greatly from the datasets used in this study.

According to the results, apart from the size of the non-permanent objects, it is observed that their proximity to windows and space configuration play roles, which will be investigated more elaborately in our future work.

https://doi.org/10.26868/25222708.2023.1132

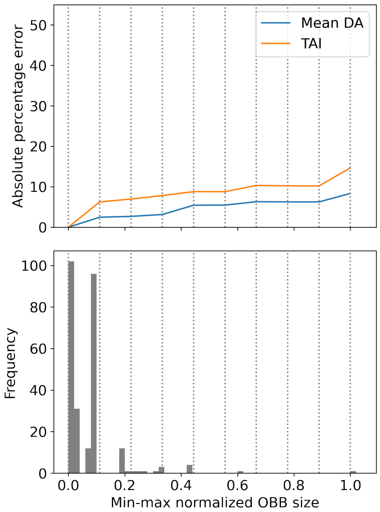

(a) S2

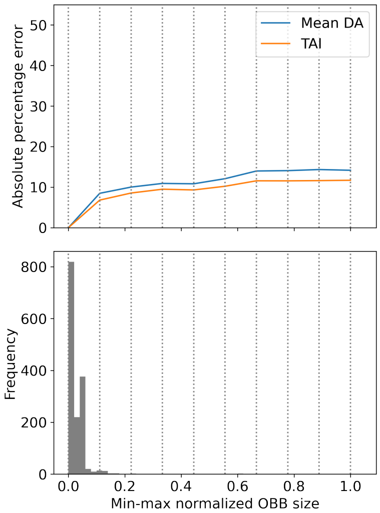

(b) S3

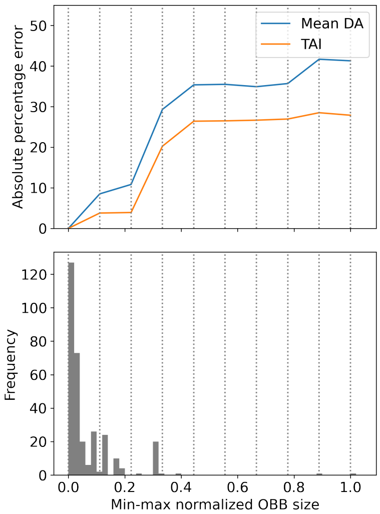

(c) S4

Figure 6: Annual daylight results for three indoor spaces

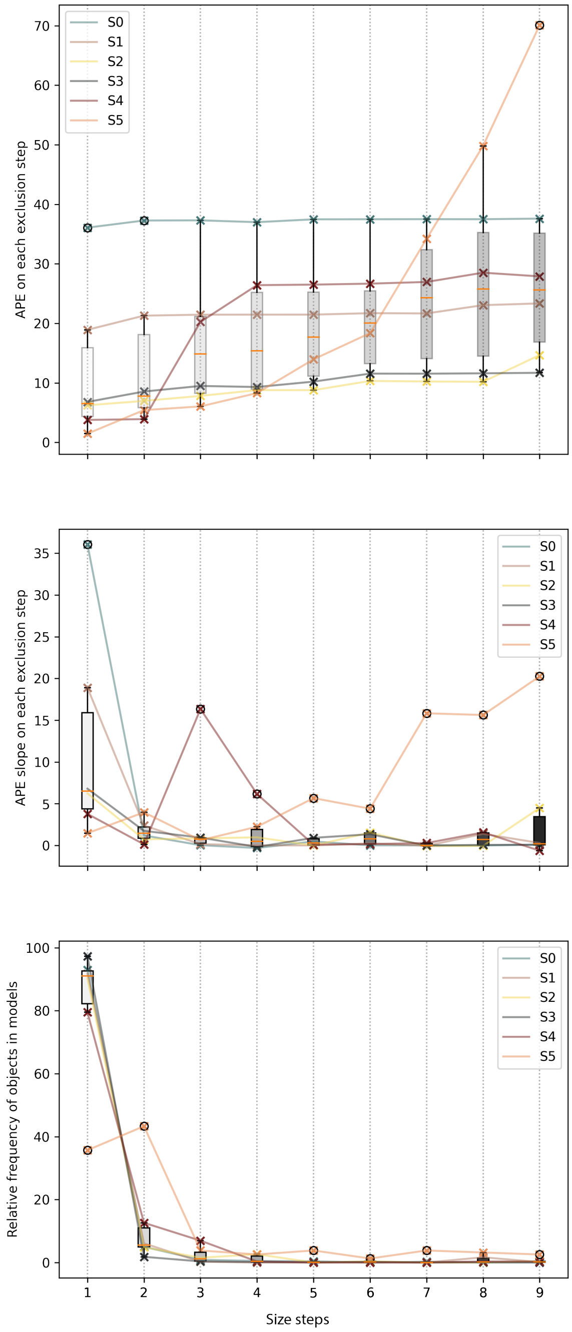

Figure 7: Summary of APE in each step (top), frequency of non-permanent objects in each step (middle), and relative frequency(bottom) across the six studied datasets for TAI.

Conclusion and future work

In this study, we measured the impacts of incremental accuracy levels for indoor 3D geometries on annual climate-based daylight results, with a focus on non-permanent indoor objects.

This impact is shown to be between 10% to 70% (APE), depending primarily on size distribution in different spaces, and the space configuration, e.g., the proximity of windows to objects, or more importantly, the size of the space. The exclusion of objects using a uniform definition of threshold, as implemented in this study, does not

https://doi.org/10.26868/25222708.2023.1132

ensure consistency across the results of different datasets, taking into account the variability of size ranges in different spaces. However, size distributions in various indoor models significantly overlap (see Fig.2). In light of this, we aim to refine the inclusion criteria to establish generalizable value ranges for similar indoor spaces.

The impact of the proximity of non-permanent objects to the windows on the errors resulting from their exclusion in the daylight model was briefly mentioned earlier. However, this aspect has not been thoroughly investigated in this study. Additionally, it is crucial to quantify the errors to gain deeper insights into the impact of using inaccurate models. This has practical implications as pre-built standard 3D models (e.g., chairs chosen from a database) are more commonly utilized than accurate 3D reconstructions from scans. These aspects will be addressed in our future research as part of the follow-up studies for this paper.

The findings of this study have practical implications for practitioners involved in indoor daylight modeling, as they can help strike a balance between the cost of modeling indoor geometry and the intended application. Furthermore, the findings of this study can inform the development of automated and semi-automated methods and pipelines for reconstructing indoor geometry from raw dense point clouds obtained through LiDAR scanning or photogrammetry. Apart from aiding in post-construction applications, this refinement is also useful for architects and engineers during the decision-making process, as it allows them to identify potential errors caused by incomplete design models.

Acknowledgement

We would like to express our sincere gratitude to Dr. Alstan Jakubiec for his generous provision of the indoor datasets used in this study.

References

Benner, J., A. Geiger, G. Gröger, K.-H. Häfele, and M.-O. Löwner (2013). Enhanced lod concepts for virtual 3d city models. In *ISPRS annals of the photogrammetry, remote sensing and spatial information sciences. Proceedings of the ISPRS 8th 3D GeoInfo conference & WG II/2 workshop*, pp. 51–61.

Biljecki, F., H. Ledoux, and J. Stoter (2016). An improved lod specification for 3d building models. *Computers, Environment and Urban Systems 59*, 25–37.

Billen, R., C. Zaki, M. Servières, G. Moreau, and P. Hallot (2012). Developing an ontology of space: Application to 3d city modeling. *Usage, Usability, and Utility of 3D City Models–European COST Action TU0801*, 02007.

Boeters, R., K. Arroyo Ohori, F. Biljecki, and S. Zlatanova (2015). Automatically enhancing citygml lod2 models with a corresponding indoor geometry. *International Journal of Geographical Information Science 29*(12), 2248–2268.

Bourgeois, D., C. F. Reinhart, and G. Ward (2008). Standard daylight coefficient model for dynamic daylighting simulations. *Building Research & Information 36*(1), 68–82.

Education Funding Agency (2014, January). *EFA Daylight Design Guide*.

EN (2019). Daylight in buildings.

Geiger, A., J. Benner, and K. H. Haefele (2015). Generalization of 3d ifc building models. In *3D geoinformation science*, pp. 19–35. Springer.

Hagedorn, B., M. Trapp, T. Glander, and J. Döllner (2009). Towards an indoor level-of-detail model for route visualization. In *2009 tenth international conference on mobile data management: systems, services and middleware*, pp. 692–697. IEEE.

Kang, H. Y., S. K. Nam, J. R. Hwang, and J. Y. Lee (2018). Lod (level of detail) model for utilization of indoor spatial data. *Journal of the Korean Society of Surveying, Geodesy, Photogrammetry and Cartography 36*(6), 545–554.

Kemec, S., S. Zlatanova, and S. Duzgun (2012). A new lod definition hierarchy for 3d city models used for natural disaster risk communication tool. In *Proceedings of the 4th International Conference on Cartography & GIS, Volume 2, Albena, June 2012, pp. 17-28*. International Cartographic Association.

Kim, J.-S., S.-J. Yoo, and K.-J. Li (2014). Integrating indoorgml and citygml for indoor space. In *International Symposium on Web and Wireless Geographical Information Systems*, pp. 184–196. Springer.

Kutzner, T., K. Chaturvedi, and T. H. Kolbe (2020). Citygml 3.0: New functions open up new applications. *PFG–Journal of Photogrammetry, Remote Sensing and Geoinformation Science 88*(1), 43–61.

Löwner, M.-O., J. Benner, G. Gröger, and K.-H. Häfele (2013). New concepts for structuring 3d city models–an extended level of detail concept for citygml buildings. In *International Conference on Computational Science and Its Applications*, pp. 466–480. Springer.

OGC (2012). City Geography Markup Language (CityGML) Encoding Standard, version: 2.0.0.

Pang, Y., Q. Yang, L. Zhou, B. Lin, and G. Lv (2020). A new level of detail concept for building indoor scene. In *IOP Conference Series: Earth and Environmental Science*, Volume 502, pp. 012020. IOP Publishing.

Quek, G. and J. A. Jakubiec (2021). Calibration and validation of climate-based daylighting models based on one-time field measurements: Office buildings in the tropics. *Leukos 17*(1), 75–90.

USGBC (2013). *LEED reference guide for building design and construction*. US Green Building Council.

https://doi.org/10.26868/25222708.2023.1132

Ward, G. J. (1994). The radiance lighting simulation and rendering system. In *Proceedings of the 21st annual conference on Computer graphics and interactive techniques*, pp. 459–472.

https://doi.org/10.26868/25222708.2023.1132